

# Measurements of Radon/Thoron Exhalation Rates and Radionuclide Contents in Muzaffarnagar Uttar Pradesh

<sup>1</sup>Vinyas Goswami and <sup>2</sup>Satendra Singh

<sup>1</sup>Research Scholar, School of Physics, Sunrise University, Alwar (R.J.)

<sup>2</sup>Associate Professor, School of Physics, Sunrise University, Alwar (R.J.)

---

## ARTICLE DETAILS

### Article History

Published Online: 16 Jan 2020

### Keywords

Soil, Radon, neo-tectonic activities, soil-gas radon concentrations.

### Corresponding Author

Email: vinyasgs@gmail.com

---

## ABSTRACT

*This research article is centered on the description of the radon mass exhalation rate measurements, along with thoron outward outbreath rate and thoron quantity discharge rate at different location of Muzaffarnagar District. Afterwards, this study also comprises the investigation of the foremost source term of radon and thoron (Thorium and Potassium content, Radionuclides Radium) in the region of Muzaffarnagar, Uttar Pradesh using gamma ray spectrometer. The analyzed Rn, Th and K gratified can be explained in terms of Radium Alike action index along with outdoor and inner fitness threat key, enthralled rate of quantity and an annual effective dose of the study area. After that correlation graphs were plotted between radon and thoron flux (surface and mass) with gamma level. At last, found the relationship b/w source terms of thoron and radon outbreath rate.*

---

## Background

According to UNSCEAR studies in 2000 and 2010, radon (<sup>222</sup>Rn) and thoron (<sup>220</sup>Rn) radionuclides evanescent from radium (<sup>226</sup>Ra, <sup>224</sup>Ra) present in the Earth's crust as intact U-238 and Th-232. described as a product. chain. Note that decay products of <sup>222</sup>Rn, <sup>220</sup>Rn and <sup>222</sup>Rn, <sup>220</sup>Rn itself account for most (52%) of the dose of ionizing radiation that directly affects the general population. Epidemiological studies have also convincingly confirmed an association between indoor Rn-222 exposure and lung cancer (Darby et al., 2005, Krewski et al., 2005). Parent gases and related decay products are found in dwellings due to the presence of parent radionuclides in building materials and soils. Concentration levels of <sup>222</sup>Rn and <sup>220</sup>Rn. A dwelling depends primarily on exhaled air from building materials, soil, etc., and then on environmental conditions such as ventilation rate, temperature, pressure and humidity. The <sup>222</sup>Rn/<sup>220</sup>Rn exhalation and emission rates (i.e., the source term) depend on parent radionuclide content, topography, rock composition, soil permeability, other geological parameters, and the local environment (Johner and Surbeck, 2001; Prasad et al., 2008). ). The <sup>222</sup>Rn and <sup>220</sup>Rn expiratory rates are defined as the release of <sup>222</sup>Rn or <sup>220</sup>Rn gas per unit mass or surface area per unit time from the soil matrix. Several survey-based studies have been conducted to report <sup>222</sup>Rn and <sup>220</sup>Rn concentrations in home and work environments (Bossew and Lettner, 2007, Eappen et al., 2006, Jelle, 2012, Kant et al., 2009, Kumar et al., 2014, Ramola et al., 2010, Ramola et al., 2013, Ramola et al., 2016, Teras et al., 2016). Relatively few studies have been performed to explore and validate the concept of source (Chau et al., 2005, Kumar et al., 2014, Mayya, 2004, Prasad et al., 2008, Ryzhakova, 2014, Tripathi et al., 2014). al., 2008) ). In our previous study (Singh. K. et al. 2016), indoor <sup>222</sup>Rn/<sup>220</sup>Rn and decay products in Muzaffarnagar district were measured only in winter. Relatively higher than normal concentrations have been reported in this area. <sup>222</sup>Rn and

<sup>220</sup>Rn enter the indoor environment through her two main processes:

- (1) pressure differences between soil gases and building air, known as advection;
- (2) the concentration gradient between soil and indoor air, known as diffusion;

Both processes are related to the natural properties of the interface (usually the concrete of the house) that separates both media. Radon diffusion through structural boundaries was generally assumed to be negligible compared to radon penetration through cracks and crevices due to pressure-driven airflow. Indoor radon concentrations are determined by a balance between the rate of entry from sources and the rate of removal, primarily through ventilation (Nazaroff and Nero, 1984). The main sources of indoor radon concentrations are the soil beneath the house, structure materials and ventilation rates.

The contribution of outside air to the total radon concentration in a home is often relatively small. Materials involved in radon transport have three main quantifiable physical properties. These factors are porosity, air permeability, and diffusion coefficient. Porosity is defined as the ratio of the void volume (air) within a material to its mass or total geometric volume. Increasing the porosity creates an air layer for radon transport within the material, thereby reducing the resistance to radon transport. A material's permeability classifies its ability to act as a barrier to the movement of radon gas in the presence of a pressure gradient across the material and is closely related to the material's porosity. The radon diffusion coefficient of a material quantifies the ability of radon gas to pass through a material when a concentration gradient is the driving force. This parameter is also closely related to porosity and permeability. Levels of natural radioactivity are altered by its formation, transport, and various chemical and biochemical interactions (ECNR 1995). Analysis of these natural

radionuclides is therefore one of the most important parameters for assessing human environmental impact. Radon is a daughter product of radium and is produced due to the presence of  $^{238}\text{U}$  in soil and rocks. Radon enters the environment through processes of exhalation and exhalation from the soil matrix (Etiopie and Martinelli, 2002). As reported by Gregory et al. 2013; Kardose et al. Variations in radon emissivity in 2015 depend on lithology and its composition. Therefore, the radon release rate at the soil surface mainly depends on the transport properties of the medium and the concentration of its parent element. In the current work, the expiratory velocity of  $^{222}\text{Rn}$  and  $^{220}\text{Rn}$  from soil samples was measured to estimate the source term. These soil samples were collected from different locations in the Muzaffarnagar district of Uttar Pradesh. Subsequently, the study also included the analysis of the most important source terms for the West Uttar Pradesh region, radon and thoron (content of the radionuclides radium, thorium, and potassium) using gamma-ray spectroscopy. Expiratory velocity was measured using standard measurement techniques and protocols, and a correlation study was performed as a follow-up study.

### Methodological Techniques

$^{222}\text{Rn}$  and  $^{220}\text{Rn}$  expiratory rate measurements were performed using the accumulator technique supported by the  $^{222}\text{Rn}/^{220}\text{Rn}$  continuous monitor (SMART RnDuo). SMART RnDuo is a commercially available portable continuous monitor for measuring  $^{222}\text{Rn}$ ,  $^{220}\text{Rn}$  and total alpha in air, soil and water. It is based on the principle of detecting alpha particles by scintillation with ZnS: Ag. Details of the detection principle and measurement protocol have been described elsewhere (Gaware et al., 2011). For the source terms radium ( $^{226}\text{Ra}$ ), thorium ( $^{232}\text{Th}$ ) and potassium ( $^{40}\text{K}$ ) measurements, soil samples were taken from similar locations where soil exhalation was performed. These samples were taken from some depth to eliminate possible surface contamination of undivided soils (IAEA, 2003). After collection, organic pebbles, roots and vegetation were separated from soil samples and all samples were ground into a fine powder. These samples were then dried in an electric oven at a temperature of  $110\text{ }^\circ\text{C}$  for 1 day and a 150 micron mesh size sieve was used to obtain fine quality sample powders. To allow long-term equilibration between  $^{226}\text{Ra}$ ,  $^{222}\text{Rn}$  and their short-lived daughter products, 250 g of dry samples were packed in airtight Marinelli cups for about one month. The Muzaffarnagar district of Uttar Pradesh was selected for these studies. Districts have different placements of structural elements and different formations with some locations skipped.

### $^{222}\text{Rn}$ mass exhalation rate from the soil samples

A soil sample of approximately 1000g was taken from a nearby living/working area. Appropriate precautions were taken to prevent matrix changes during the soil sampling process. The Smart RnDuo is connected to a closed collection chamber with a sample capacity of approximately 500 g. The chamber consists of an 8 cm high, 10 cm diameter stainless steel cylinder connected at the top to a photomultiplier tube connected to a Lucas cell. For  $^{222}\text{Rn}$  measurements, SMART Duo was used in diffuse mode to

avoid  $^{220}\text{Rn}$  interference (if present on the ground). The increase in  $^{222}\text{Rn}$  concentration in the accumulation chamber was measured hourly until saturation.  $^{222}\text{Rn}$  concentration data were plotted against elapsed time. The radon increase over time in units of Bq/m<sup>3</sup> in the storage chamber is obtained from the exponential equation (Aldenkamp et al., 1992).

$$C(t) = \frac{J_m M}{V \lambda_e} [1 - e^{-\lambda_e t}] + C_0 e^{-\lambda_e t} \quad (1.1)$$

$\lambda_e$  represents the active decay persistent (h-1), which is the summation of the  $^{222}\text{Rn}$  decay constant and the accumulator leak rate (if any), and  $C_0$  is the initial  $^{222}\text{Rn}$  concentration in the chamber at  $t=0$ . You can fit the exponential decay equation in Origin software. Equation:  $Y = Y_0 + A e^{-x/t_1}$

$$(1.2)$$

By comparing equation 4.1 and 4.2, we can get the  $^{222}\text{Rn}$  mass exhalation rate as

$$J_m = \frac{V_0 V \lambda_e}{M}$$

And active decay persistent  $1/t_1 = \lambda_e$

### Soil sample $^{220}\text{Rn}$ surface exhalation rate

$^{220}\text{Rn}$  surface expiratory velocity from the collected samples was measured by the same closed collection chamber technique. Due to the short diffusion distance in air (2-3 cm), the distribution of  $^{220}\text{Rn}$  in the accumulator is not uniform. However, the homogeneity of the  $^{220}\text{Rn}$  distribution can be maintained in flow mode.  $^{220}\text{Rn}$  sampling from the accumulator was performed in flow-through mode in a closed-loop setup. In flow mode, Smart Rn Duo with built-in functionality automatically turns the pump on for 5 minutes on 15 minute cycles or 15 minutes on 60 minute cycles. During expiratory rate measurements of  $^{220}\text{Rn}$ , the air volume in the chamber was minimized to ensure complete air mixing within the closed circuit. Detailed measurement principles have been extensively discussed in the literature (Gaware et al., 2011). Four measurements were averaged to estimate the steady-state  $^{220}\text{Rn}$  concentration CT (Bq/m<sup>3</sup>) in the accumulator. The CT values were then used to estimate the  $^{220}\text{Rn}$  surface expiratory velocity using the mass balance-based formula (1.3) (Sahoo and Mayya, 2010).

$$J_s = \frac{C_T V \lambda}{A} \quad (1.3)$$

Where  $J_s$  is the superficial release rate of  $^{220}\text{Rn}$  from the soil (Bq/m<sup>2</sup>/h), V is the volume confined in the closed loop (m<sup>3</sup>),  $\lambda$  (0.012464 s<sup>-1</sup>) is the decay constant of  $^{220}\text{Rn}$ , A is the cross-sectional area of the chamber (m<sup>2</sup>).

### $^{220}\text{Rn}$ mass emanation rate from the soil samples

The  $^{220}\text{Rn}$  mass discharge degree from the soil samples can be obtained using equation (4.4) (Celikovi et al., 2008).

$$J_m = \frac{J_s}{\rho L_s} \tanh \frac{Z_s}{L_s}$$

where  $Z_s$  is the height of the sample in the chamber,  $L_s$  is the  $^{220}\text{Rn}$  diffusion length in the soil, and  $\rho$  is the density of the

soil sample.  $J_s$  is the  $^{220}\text{Rn}$  surface exhalation velocity obtained from equation (1.3). The diffusion distance of  $^{220}\text{Rn}$  in soil is about 1 cm (Mayya, 2004) and the  $Z_s/L_s$  ratio can be much larger than one. With this approximation, equation (1.4) can be written as

$$J_m = \frac{J_s}{\rho L_s}$$

Equation (1.5) may be written as to assess the  $^{220}\text{Rn}$   $J_m$  (mass emanation) rate.

### Gamma Ray Spectrometry

Prepared soil illustrations were sited in the fortification unit of  $\gamma$ -ray spectrometry aimed at a 3-hour period. The assessment of natural radionuclides present in said soil samples were carried out by using Scintillation NaI (TI)  $\gamma$  particle emission indicators of dimension 63X63 mm with an analyzer which have multiple channel.

### Energy Calibration

The gamma-ray spectrometer energy was calibrated at an energy of 661 keV against a  $^{137}\text{Cs}$  source available from Atomtex, Belarus. Calibrated energy peaks identified 1460 keV at 40K,  $^{226}\text{Ra}$  activity from the 1764 keV analysis was performed with  $^{214}\text{Bi}$  gamma rays, and  $^{232}\text{Th}$  activity with  $^{208}\text{Tl}$  2620 keV gamma rays. The radioactivity of  $^{226}\text{Ra}$  and  $^{232}\text{Th}$  was evaluated using 1764 keV gamma rays from  $^{214}\text{Bi}$  and 2610 keV gamma rays from  $^{208}\text{Tl}$ , respectively. Similarly, the 40K activity was assessed by its own 1460 keV photoppeak. Energy calibration of the spectrometer was performed at 661 keV from a manufacturer-provided  $^{137}\text{Cs}$  point source, limiting the energy resolution to 9.5%.

To reduce the contribution of background radiation, spectra were also analyzed without the source (or sample) and the background (activity) counts were excluded from the recorded sample counts to obtain the net sample (activity) counts. The detector system was shielded with a lead absorber to reduce background radiation from the environment. Gamma spectral analysis was performed by SPTR – ATC (AT-1315) radiology computer software.

### Equivalent Activity Index of Radium

Radionuclides ( $^{226}\text{Ra}$ ,  $^{232}\text{Th}$ , and  $^{40}\text{K}$ ) are not evenly distributed in soil and rocks. A generic radiation index was introduced to express the activity levels of these radionuclides in a single quantity that takes into account the associated radiation damage (Diab et al., 2008). This measure is called radium equivalent (Raeq) radioactivity and is defined mathematically (Ramola et al., 2008a; UNSCEAR 2000).

$$R_{\text{aeq}} = 0.077A + A_{\text{Ra}} + 1.43 A_{\text{Th}} \quad (1.6)$$

Wherever the commotion concentrations of  $^{232}\text{Th}$ ,  $^{226}\text{Ra}$  and 40K are  $A_{\text{Th}}$ ,  $A_{\text{Ra}}$ , also  $A_{\text{K}}$ , respectively.

### Hazard Index of External and Internal Health (Hex and Hin)

The external hazard index is a measure of natural gamma ray hazards (Ibrahim, 1999). The main purpose of this index is to limit the radiation dose to a permissible dose equivalent of 1

mSv-1 (ICRP, 1991). To evaluate this exponent, you can use the following formula:

$$\text{Hex} = \frac{A_{\text{Ra}}/370 + (A_{\text{Th}}/259) + (A_{\text{K}}/4810)}{1} \quad (1.7)$$

Respiratory alpha particles emitted from the short-lived radionuclides radon (a daughter product of  $^{226}\text{Ra}$ ) and thoron (a daughter product of  $^{232}\text{Th}$ ) is also harmful to the respiratory system. This hazard can be quantified by the internal hazard index ( $H_{\text{in}}$ ) given by (Quinods et al., 1987).

$$H_{\text{in}} = \frac{A_{\text{Ra}}/185 + (A_{\text{Th}}/259) + (A_{\text{K}}/4810)}{1} \quad (1.8)$$

$A_{\text{Th}}$ ,  $A_{\text{Ra}}$ , and  $A_{\text{K}}$  are the radioactivity concentrations of  $^{226}\text{Ra}$ ,  $^{232}\text{Th}$ , and 40K in Bqkg-1, respectively.

### Absorbed Dose Rate (D)

According to UNSCEAR (2000) guidelines, the outdoor absorbed dose rate (D) from airborne gamma rays 1 m above the ground was uniform for the distribution of naturally occurring radionuclides ( $^{226}\text{Ra}$ ,  $^{232}\text{Th}$ , and 40K). Calculated the conversion factors used to calculate the absorbed Y dose rate (D) in air per activity concentration of Bqkg-1 are 0.462  $\mu\text{Gy} \cdot \text{h}^{-1}$  for  $^{226}\text{Ra}$  (for the U series), 0.621  $\mu\text{Gy} \cdot \text{h}^{-1}$  for  $^{232}\text{Th}$ , and 0.0417  $\mu\text{Gy} \cdot \text{h}^{-1}$  at 40K (UNSCEAR, 2000), given according to the following relations:

$$D (\mu\text{Gy} \cdot \text{h}^{-1}) = 0.462A_{\text{Ra}} + 0.604A_{\text{Th}} + 0.0417A_{\text{K}} \quad (1.9)$$

### Effective Dose on the bases of Annual

To estimate the annual average effective dose equivalent received by members, we convert the absorption rate to human effective dose equivalent using a conversion factor of 0.7 SvGy-1. Indoor and outdoor occupancy is 80% and 20% respectively (UNSCEAR, 1993). The determination of the annual effective dose is:

$$\text{Internal (mSv)} = \text{Immersed Dose (nGy} \cdot \text{h}^{-1}) \times 8760 \times 0.7 \text{ SvGy}^{-1} \times 10^{-6} \times 0.8 \quad (1.10)$$

$$\text{Al fresco (mSv)} = \text{Immersed Dose (nGy} \cdot \text{h}^{-1}) \times 8760 \times 0.7 \text{ SvGy}^{-1} \times 10^{-6} \times 0.2 \quad (1.11)$$

### Result and Discussion

In this study, radon mass emission rate, thoron surface emission rate, and thoron mass emission rate were measured after constructing a correlation diagram at the gamma-ray level in Muzaffarnagar District, Uttar Pradesh. Once the river survey was completed, these samples were analyzed to determine the distribution of radionuclides ( $^{226}\text{Ra}$ ,  $^{232}\text{Th}$ , and 40K) in these areas. Analytical results of radionuclides ( $^{226}\text{Ra}$ ,  $^{232}\text{Th}$ , and 40K) were used to calculate radium equivalent (Raeq), external and internal health hazard indices (Hex and Hin), absorbed dose rate (D), and annual effective dose. Indoor and outdoor spaces for measuring the study area were further analyzed (Muzaffarnagar District).

### $^{222}\text{Rn}$ and $^{220}\text{Rn}$ exhalation rate from the collected soil in Muzaffarnagar District

For exhalation and shedding rate analysis, 50 soil samples were collected from different locations in Muzaffarnagar

District and selected based on background gamma values. Of these, 24 soil samples were collected in Muzaffarnagar District. The mean and standard deviation of gamma ray level, <sup>222</sup>Rn mass ejection rate, <sup>220</sup>Rn surface ejection rate and <sup>220</sup>Rn mass ejection rate are shown in Table 4.1.

The mass expiratory rate for <sup>222</sup>Rn varied from 16±1 to 54±1 mBq/kg/h with an arithmetic mean (standard deviation) of 30±10 mBq/kg/h, while the surface expiratory rate for <sup>220</sup>Rn

varied from 0.66 to It was in the range of 6.43 Bq/h. The arithmetic mean (standard deviation) of m<sup>2</sup>/s was 2.18±1.36 Bq/m<sup>2</sup>/s. As shown in Table 1.2, higher levels of <sup>222</sup>Rn bulk exhalation (indicated by site codes S3, S4, S8, and S18) can be associated with high levels of radium (<sup>226</sup>Ra) in soil. Similarly, at sites with codes S3, S4, S15 and S21, we observed higher values of <sup>220</sup>Rn expiratory rate attributed to higher thorium content (<sup>232</sup>Th) compared to other selected sites.

**Table 1.1: γ levels, expiratory rates of <sup>220</sup>Rn and <sup>222</sup>Rn, and mass exhalation rates of <sup>220</sup>Rn measured in soil samples from Muzaffarnagar district**

Location	code of Location	γ- levels(μSv/h)	<sup>222</sup> Rn mass outbreak rate (mBq/kg/h)	<sup>220</sup> Rn surface outbreak rates (Bq/m <sup>2</sup> /s)	<sup>220</sup> Rn mass emanation rates (mBq/kg/s)
Badhiwala	S1	0.2±0.02	32±1	1.12±0.01	134
Akbargarh	S2	0.12±0.01	18±1	1.60±0.23	191
Dhudhli	S3	0.31±0.03	54±1	6.43±0.04	769
Ali Pura	S4	0.2±0.01	54±2	3.95±0.03	472
Almaspur	S5	0.2±0.02	29±2	1.01±0.02	120
Badheri	S6	0.16±0.02	36±1	2.23±0.02	267
Badiwala	S7	0.13±0.01	35±1	1.23±0.11	148
Baghra	S8	0.1±0.01	46±2	1.36±0.03	163
Bagowali	S9	0.16±0.02	19±1	3.87±0.21	462
Tugalakpur	S10	0.27±0.02	24±2	2.32±0.15	277
Khorkee	S11	0.19±0.02	21±1	1.75±0.05	209
Balwakheri	S12	0.17±0.01	39±1	2.13±0.11	254
Bamanheri	S13	0.15±0.01	20±1	1.63±0.23	195
Charthawal Rural	S14	0.15±0.02	16±1	0.65±0.02	78
Dadupur	S15	0.24±0.03	26±2	3.52±0.14	421
Dhandhera	S16	0.19±0.02	19±1	1.18±0.12	141
Dhudhli	S17	0.19±0.02	40±1	1.03±0.42	123
Faridpur	S18	0.19±0.01	42±1	2.23±0.27	267
Jaroda	S19	0.2±0.03	31±1	2.81±0.34	336
Kalewala	S20	0.14±0.02	26±1	3.08±0.41	369
Lakhnauti	S21	0.16±0.01	24±1	3.72±0.36	445
Mandi	S22	0.17±0.02	33±1	0.90±0.002	108
Mirzapur	S23	0.2±0.03	25±1	1.55±0.02	185
Nuna Khera	S24	0.12±.01	27±1	1.04±0.03	124

The mass expiratory rate for <sup>222</sup>Rn varied from 16±1 to 54±1 mBq/kg/h with an arithmetic mean (standard deviation) of 30±10 mBq/kg/h, while the surface expiratory rate for <sup>220</sup>Rn varied from 0.66 to It was in the range of 6.43 Bq/h. The arithmetic mean (standard deviation) of m<sup>2</sup>/s was 2.18±1.36 Bq/m<sup>2</sup>/s. As shown in Table 4.2, higher levels of <sup>222</sup>Rn mass exhaled air (indicated by site codes S3, S4, S8, and S18) can

be associated with high levels of radium (<sup>226</sup>Ra) in soil. Similarly, at sites with codes S3, S4, S15 and S21, we observed higher values of <sup>220</sup>Rn expiratory rate attributed to higher thorium content (<sup>232</sup>Th) compared to other selected sites. <sup>226</sup>Ra and <sup>232</sup>Th levels in soil samples measured by gamma spectrometry are shown in Table 1.2.

**Table 1.2: <sup>226</sup>Ra, <sup>232</sup>Th and <sup>40</sup>K radionuclides and annual effective doses measured in soil samples (Muzaffarnagar District)**

Location Code	Activity Concentration Bqkg <sup>-1</sup> (concentration±Ra <sub>eq</sub> (Bqkg <sup>-1</sup> error)			Health Hazard Index	Absorbed Dose (nGyh <sup>-1</sup> )	Annual Effective Dose (mSv)			
	<sup>226</sup> Ra	<sup>232</sup> Th	<sup>40</sup> K			Hex	H <sub>in</sub>	Indoor	Outdoor
S1	62±10	36±8	2018±245	268	0.72	0.89	134	0.66	0.16
S2	44±8	48±8	1937±253	262	0.71	0.83	130	0.64	0.16

S3	91±12	89±11	2165±276	385	1.04	1.29	186	0.91	0.23
S4	70±10	38±7	1991±256	277	0.75	0.94	138	0.68	0.17
S5	39±8	34±7	2003±257	242	0.65	0.76	122	0.60	0.15
S6	52±5	48±8	1995±226	275	0.74	0.88	136	0.67	0.17
S7	37±9	54±9	1987±258	268	0.72	0.82	133	0.65	0.16
S8	46±9	44±8	2135±273	273	0.74	0.86	137	0.67	0.17
S9	62±5	68±7	2443±285	347	0.94	1.10	172	0.84	0.21
S10	39±8	27±7	1957±251	229	0.62	0.72	116	0.57	0.14
S11	38±10	31±5	1882±255	228	0.62	0.72	115	0.56	0.14
S12	55±9	63±9	1844±245	287	0.78	0.92	140	0.69	0.17
S13	38±8	40±9	2004±258	250	0.68	0.78	126	0.62	0.15
S14	48±9	42±8	2036±262	264	0.71	0.84	132	0.65	0.16
S15	43±8	49±7	2341±263	293	0.79	0.91	147	0.72	0.18
S16	39±8	27±8	1957±251	229	0.62	0.72	116	0.57	0.14
S17	52±9	52±9	1877±255	271	0.73	0.87	134	0.66	0.16
S18	41±9	39±8	2215±279	267	0.72	0.83	135	0.66	0.17
S19	56±8	49±7	2441±289	314	0.85	1.00	157	0.77	0.19
S20	39±9	42±10	1889±264	245	0.66	0.77	123	0.60	0.15
S21	41±6	49±6	2054±260	269	0.73	0.84	134	0.66	0.16
S22	37±8	29±8	1857±261	222	0.60	0.70	112	0.55	0.14
S23	41±9	47±8	2057±272	267	0.72	0.83	133	0.65	0.16
S24	38±9	31±11	2100±260	244	0.66	0.76	124	0.61	0.15

The <sup>226</sup>Ra, <sup>232</sup>Th values obtained at these locations are relatively higher than the global average values (35, 30, and 400) Bq/kg for <sup>226</sup>Ra, <sup>232</sup>Th, and <sup>40</sup>K (OECD 1979). Potassium (<sup>40</sup>K) was found to be slightly higher than the stated global values due to Indian geological formations and topography (Kumar et al., 2015). Differences in the release rates of <sup>222</sup>Rn and <sup>220</sup>Rn can also be attributed to differences in geological distribution and soil composition. Expiratory velocities in the study area are expected to be greatly influenced by these thrust formations and local faults. To visualize the distribution patterns, the frequency distributions of the measured <sup>222</sup>Rn and <sup>220</sup>Rn expiratory rates are also shown in Figure 1. 4.1 or Fig. 4.2. A frequency distribution plot of the <sup>222</sup>Rn mass expiratory rate indicates

that about 11 of the 24 soil samples had a <sup>222</sup>Rn mass expiratory rate of 20-30 mBq/kg/h and two soil samples had a <sup>222</sup>Rn mass expiratory rate of about 50-60 mBq/kg/h. indicates that it has a higher value. h. The high value is due to the high radium grade compared to various other locations and strata (see Table 1.2). Figures 1.1 and 1.2 are pictorial graphs showing the expiratory velocity of collected soil samples. In the case of <sup>220</sup>Rn surface expiratory rate, high expiratory rate was detected in the same soil samples that obtained high <sup>222</sup>Rn bulk expiratory rate. Both radon and thoron emissions are independent processes, but monazite sands are radioactive due to the presence of thorium and, less commonly, uranium. Higher thoron grades are expected in monazite regions that predict thorium deposits.

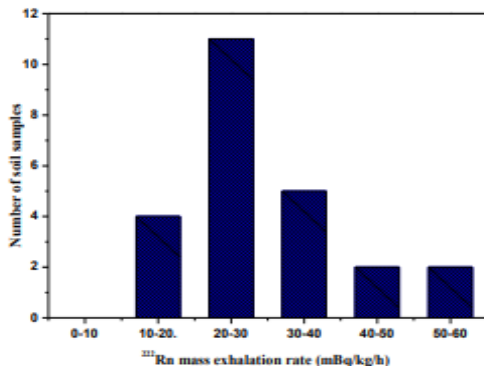


Fig. 1.1: Frequency distribution of <sup>222</sup>Rn mass outbreak rate

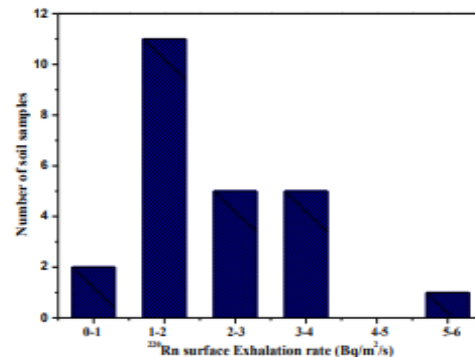


Fig. 1.2: Incidence distribution of <sup>220</sup>Rn surface outbreak rate

To further the observation, a correlation diagram between expiratory rates of <sup>222</sup>Rn and <sup>220</sup>Rn was drawn (see Figure 1.3). Surprisingly, the correlation coefficient is 0.21, indicating a weak positive correlation between the two. This is due to

the distribution of their parent source terms (<sup>226</sup>Ra and <sup>232</sup>Th, respectively) and soil composition, which is expected to be uncorrelated.

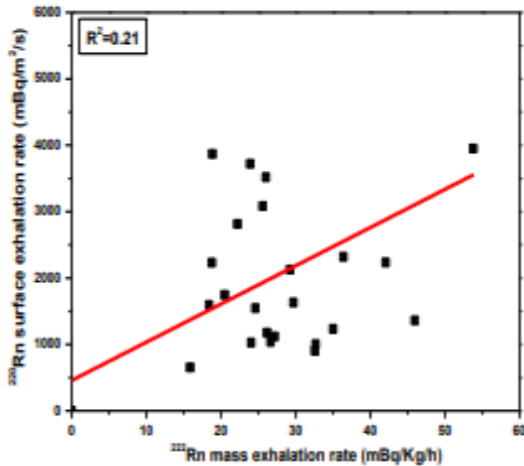


Fig. 1.3: Correlation between 222Rn and 220Rn exhalation rate

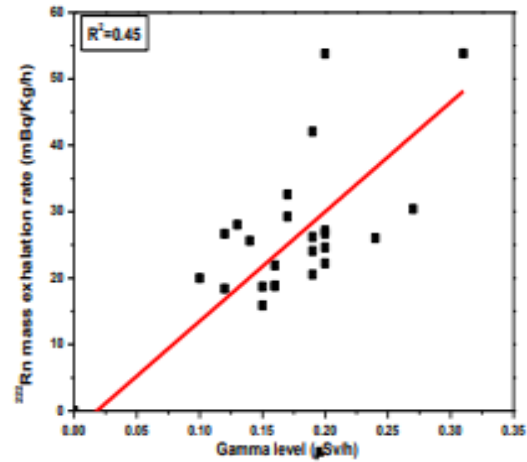


Fig. 1.4: Correlation between 222Rn outbreak rate and  $\gamma$ -level

**222Rn and 220Rn outbreak rate and Gamma exposure**

Figure 1.4 shows the correlation between gamma levels and 222Rn mass exhalation rate, which also shows a weak positive correlation (correlation coefficient 0.45). Similarly, Figure 1.5 also shows a weak positive correlation (correlation coefficient 0.33) between gamma level and 220Rn exhalation rate.

This is due to the higher mobility of 222Rn/220Rn in the vicinity than the 226Ra and 232Th contents in soil. Furthermore, collected soil samples representing different locations have different shapes and particle sizes (soil composition), which determine and influence the release rate of 222Rn/220Rn from soils.

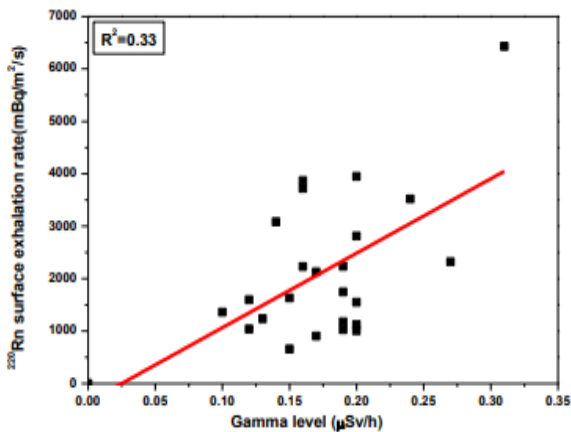


Fig. 1.5: Correlation between 220Rn surface exhalation and Gamma level

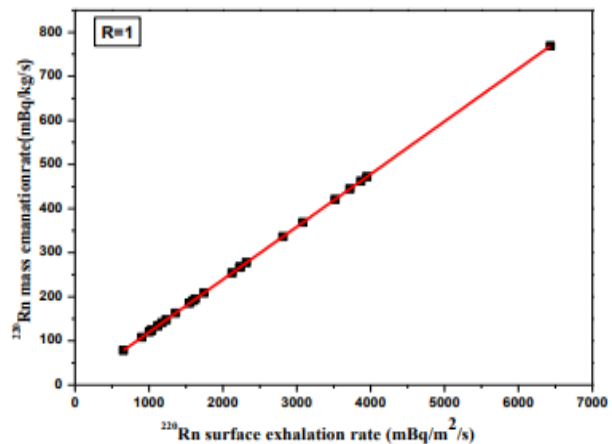


Fig 1.6: Correlation between surface exhalation and emanation rate of 220Rn

**220Rn exhalation rate and 220Rn mass ejection rate**

220Rn mass release rates (mBq/kg/s) from various soil samples collected from various locations are shown in Table 1.1. Emission coefficients varied from 78 to 769 mBq/kg/s, averaging 251±161 mBq/kg/s. Figure 1.6 shows the correlation between the mass release rate of 220Rn and the exhalation rate. It is observed that the higher the 220Rn release rate, the higher the 220Rn mass release rate, thus showing a strong positive correlation with R=1 (Table 1.1).

**Distribution of natural radionuclides**

Fifty soil samples were taken from the study area (Muzaffarnagar district) to determine the content of radium, thorium and potassium. The 222Rn and 220Rn mass exhalation rates were measured for these soil samples, as

shown in Tables 1.1 and 1.3, respectively. In the Muzaffarnagar area, 226Ra, 232Th and 40K levels in soil samples ranged from 37±9 Bq/kg to 91±12 Bq/kg with mean values of 48 Bq/kg and 27±7 Bq/kg to 89, varying from ±11 Bq/kg with a mean of 45 Bq/kg and from 1844±245 Bq/kg to 2443±285 Bq/kg with a mean of 2049 Bq/kg. As shown in Figure 1.7, there is a strong correlation between the mass ejection rate of 222Rn and its radium content (correlation coefficient R2 = 0.88). Similar observations were found for the surface release rate of 220Rn and its thorium content (correlation coefficient R2 = 0.82), as shown in Figure 1.8. This is due to their geological formation, lithology (mylonitized porphyritic granite, quartz porphyry, granite gneiss) and high mobility of 222Rn and 220Rn gases to the surface. The average values of 226Ra and 232Th in

the Muzaffarnagar region were slightly above the global average. H. 50 BqKg-1 or 10-50 BqKg-1. The study area average of 40,000 exceeds the limit given by UNSCEAR (2000). H. 100-700 Bqkg-1. Radium equivalent radioactivity (R<sub>eq</sub>) was found to vary between 222 Bqkg-1 and 384 Bqkg-1 with an average value of 270 Bqkg-1. The average radium equivalent radioactivity was below the recommended

value of 370 Bqkg-1 (OECD, 1979). These high values of 226Ra, 232Th, and 40K are associated with uranium, thorium mineralization, and highly mylonitized zones of porphyry, granite, quartz porphyry, shale, phyllite, schist, and quartzite. It may be due to presence, generally indicating higher radiation levels in the research area.

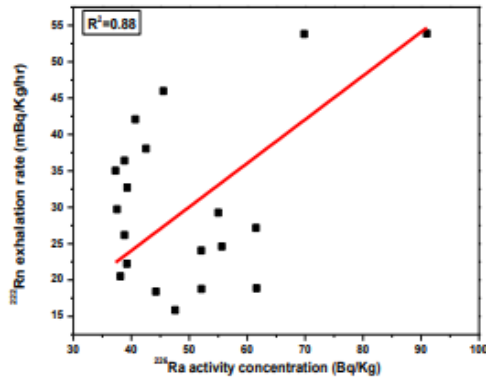


Fig 1.7: Correlation between <sup>222</sup>Rn outbreak rate and content of Radium

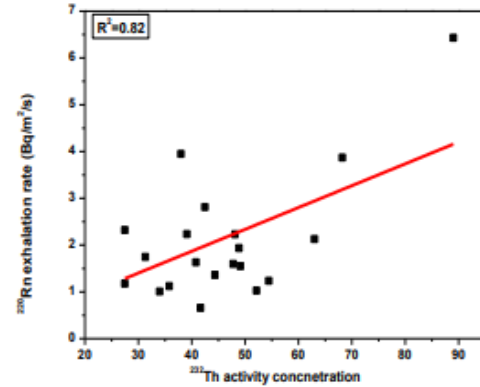


Fig 1.8: Correlation between <sup>222</sup>Rn outbreak rate and content of thorium

The external and internal health hazard index values found ranged from 0.60 to 1.04 with a mean of 0.73 and from 0.70 to 1.29 with a mean of 0.86, respectively. The average external and internal health hazard index is less than 1, which is very satisfactory and within the protection limits of the study area (UNSCEAR 1993; 2000). On the other hand, very few samples show a health hazard index greater than 1. The total absorbed dose rate was found to vary between 112 nGyh-1 and 186 nGyh-1 with an average value of 135 nGyh-1 due to the presence of 226Ra, 232Th and 40K in soil samples. Average absorbed dose rates in the study area were found to be higher than recommended. H. 60 nGyh-1 (UNSCEAR, 2000). The total effective indoor dose was found to vary between 0.55 mSvy-1 and 0.91 mSvy-1, with an average value of 0.66 mSvy-1. The total effective outdoor dose was found to vary between 0.14 mSvy-1 and 0.23 mSvy-1, with an average value of 0.17 mSvy-1. The high concentration of 226Ra in the study area (Muzaffarnagar) may be due to the presence of high uranium grade ores deposited in the rocks of the study area. Similar trends of high radioactivity in granite have been reported by other researchers (Omran, 2005; Anjos et al., 2005; El-Arabi, 2007). A variety of commonly found granular flat phosphates, composed of fragments of associated rock units, suggest simultaneous transport and turbulence within the basin. The apatite layer varies in thickness from about 1m to 5m, but radioactivity is confined to the lowest 0.3m to 1.5m thickness of the formation. Radioactivity variability strongly depends on the geological conditions of the study area and the composition of the rock formations in this area (Choubey et al., 1999). Absorbed dose rates to air and other radiation effects at 1 m above the ground were calculated when these soil samples were used as building materials on a local scale. These results are also important for environmental studies, as local soils in the hill

country are used for a variety of purposes in mud houses. External and internal health hazard indices were calculated from the measured radioactivity in terms of radiation protection. Respiratory rate of 222Rn and 220Rn from soil sampled in Muzaffarnagar district

For expiratory and expiratory rate analyses, 50 soil samples selected by measuring background gamma values were collected from different locations in Muzaffarnagar District. Of these, 26 soil samples were collected in Muzaffarnagar District. Gamma-ray values, 222 Rn mass emission rate, 220 Rn surface emission rate, and 220 Rn mass emission rate were summarized using the mean values and standard deviations shown in Table 1.3. From Table 1.3, the mass expiratory rate for 222Rn varies from 13 to 81 mBq/kg/h with an arithmetic mean (standard deviation) of 27±9 mBq/kg/h, while the surface expiratory rate for 220Rn is 0.32 from 3.93 Bq/m<sup>2</sup>/s with an arithmetic mean (standard deviation) of 1.60±1.12 Bq/m<sup>2</sup>/s. As shown in Table 4.4, higher levels of 222Rn mass exhaled air (indicated by site codes S3 and S8) can be associated with high levels of radium (226Ra) in soil. Similarly, slightly higher values of 220Rn expiratory rate were found at the code S4 site. This is due to the higher thorium content (232Th) compared to other selected sites. High concentrations of 222Rn and 220Rn can directly bind to their parent radionuclides 226Ra and 232Th. 226Ra and 232Th levels in soil samples measured by gamma spectrometry are shown in Table 4.4. The values of 226Ra, 232Th obtained at these sites are relatively higher than the global averages of 226Ra, 232Th and 40K (35, 30 and 400 Bq/kg) (OECD, 1979). Potassium (40K), as well as the Muzaffarnagar area, has global values slightly higher than those mentioned (Kumar et al. 2015) due to Indian geological formations (Kumar et al. 2015). I found that the average value is lower than Muzaffarnagar district.

**Table 1.3  $\gamma$ -level,  $^{220}\text{Rn}$  and  $^{222}\text{Rn}$  exhalation rates and  $^{220}\text{Rn}$  mass discharge rate measured from soil samples from Muzaffarnagar district**

Location Name	Location code	Gamma levels( $\mu\text{Sv/h}$ )	$^{222}\text{Rn}$ mass exhalation rate (mBq/kg/h)	$^{220}\text{Rn}$ surface exhalation rates (Bq/m <sup>2</sup> /s)	$^{220}\text{Rn}$ mass emanation rates (mBq/kg/s)
Badhiwala	S-1	0.19±0.01	23±1	1.29±0.14	154
Akbargarh	S-2	0.16±0.02	25±0.4	0.96±0.06	115
Dhudhli	S-3	0.14±0.01	48±1	1.2±0.01	143
Ali Pura	S-4	0.14±0.02	17±1	3.58±0.23	428
Almaspur	S-5	0.16±0.01	13±0.2	1.69±0.04	202
Badheri	S-6	0.16±0.01	25±1	2.57±0.22	307
Badiwala	S-7	0.12±0.01	25±1	2.02±0.19	241
Baghra	S-8	0.22±0.03	81±1	1.88±0.15	225
Bagowali	S-9	0.15±0.02	25±1	1±0.11	119
Tugalakpur	S-10	0.17±0.01	21±1	0.32±0.03	39
Khorkee	S-11	0.19±0.02	18±1	0.47±0.21	56
Balwakheri	S-12	0.22±0.02	26±2	2.86±0.15	342
Bamanheri	S-13	0.17±0.01	32±1	0.41±0.05	49
Charthawal Rural	S-14	0.18±0.02	17±1	0.58±0.01	69
Dadupur	S-15	0.22±0.03	16±1	0.37±0.03	44
Dhandhera	S-16	0.15±0.01	30±1	0.52±0.02	63
Dhudhli	S-17	0.15±0.01	38±2	0.76±0.14	91
Faridpur	S-18	0.21±0.02	26±1	0.69±0.12	83
Jaroda	S-19	0.13±0.01	23±1	3.75±0.42	449
Kalewala	S-20	0.17±0.02	19±1	3.93±0.37	470
Lakhnauti	S-21	0.15±0.01	16±1	0.48±0.02	57
Mandi	S-22	0.20±0.02	31±1	2.75±0.41	329
Mirzapur	S-23	0.19±0.02	27±1	2.12±0.36	253
Nuna Khera	S-24	0.21±0.03	30±1	1.99±0.13	238
Pilakhni	S-25	0.18±0.02	24±1	1.66±0.19	198
Shahpur	S-26	0.18±0.02	26±1	1.99±0.16	238

Therefore, we found that the stratum (Muzaffarnagar geology) rises from Muzaffarnagar (towards the Muzaffarnagar district) due to a very high shift in expiratory velocity and radionuclide variability. This variation is due to expiratory rates of  $^{222}\text{Rn}$  and  $^{220}\text{Rn}$  caused by differences in geological distribution and soil composition. To visualize the distribution patterns, the frequency distributions of the measured  $^{222}\text{Rn}$  and  $^{220}\text{Rn}$  expiratory rates are also plotted in Figures 1.9 and 1.10. A frequency plot of  $^{222}\text{Rn}$  mass expiratory rate shows that most soil samples are between 20 and 30 mBq/kg/h. Both  $^{222}\text{Rn}$  and  $^{220}\text{Rn}$  expiratory rates resulted in fewer soil samples at higher radioactivity concentrations (see Figures 1.9 and 1.10). Since there are no barriers on the ground, radon and thoron

can easily escape into the indoor environment. Thoron diffuses within 5 cm to 20 cm from the top layer of the mud house. Mud and soil are rich sources of radioactive content. Therefore, certain locations have been identified as having high emission rates of radon and thoron due to their radioactivity levels. To further classify our observations, we constructed a correlation plot between expiratory rates of  $^{222}\text{Rn}$  and  $^{220}\text{Rn}$  (see Figure 1.11). There is a nearly strong positive correlation between them with a correlation coefficient of 0.54. This is due to the distribution of parent source terms ( $^{226}\text{Ra}$  and  $^{232}\text{Th}$ , respectively) and soil composition that are expected to be correlated.

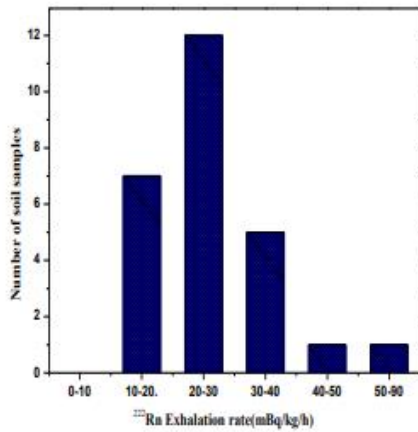


Fig. 1.9: Regularity supply of <sup>222</sup>Rn mass outbreak rate

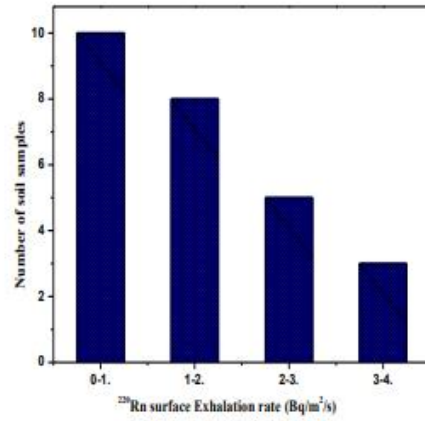


Fig 1.10: Regularity supply of <sup>220</sup>Rn surface outbreak rate

<sup>222</sup>R/<sup>220</sup>Rn outbreak rate and  $\gamma$  exposure

At selected locations in Muzaffarnagar district, gamma radiation levels were measured for correlation with exhalation rate. Figure 1.12 shows a strong correlation between gamma levels and <sup>220</sup>Rn mass expiratory rate (correlation coefficient 0.80). This strong positive correlation indicates that the flux is strongly contributed by the radium content.

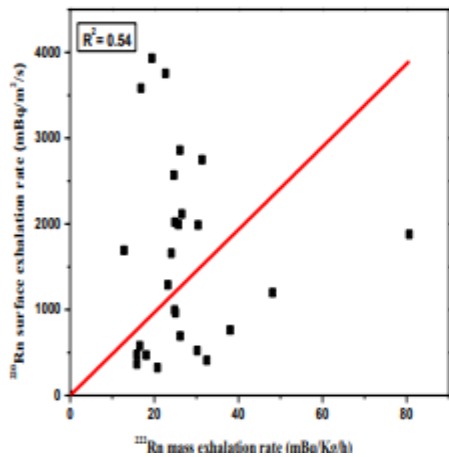


Fig.1.11: Correlation between <sup>222</sup>Rn and <sup>220</sup>Rn exhalation rate

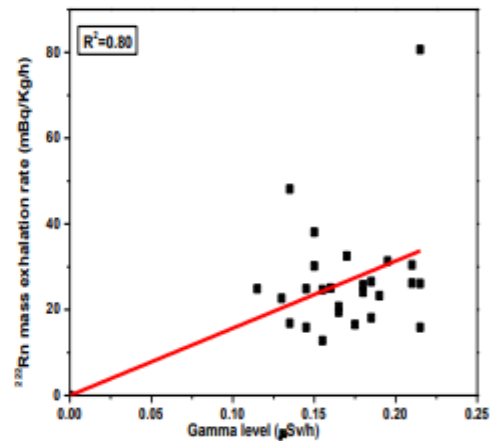


Fig. 1.12: Correlation between <sup>222</sup>Rn exhalation rate and Gamma level

present in the topsoil. Similarly, Figure 1.13 also shows a strong positive correlation (correlation coefficient 0.64) between gamma level and <sup>220</sup>Rn expiratory rate. This is due to the higher mobility of <sup>222</sup>Rn/<sup>220</sup>Rn in the vicinity than the <sup>226</sup>Ra and <sup>232</sup>Th contents in soil. Furthermore, collected soil

samples representing different locations have different shapes and particle sizes (soil composition), which determine and influence the expiratory rate of <sup>222</sup>Rn and <sup>220</sup>Rn from the soil.

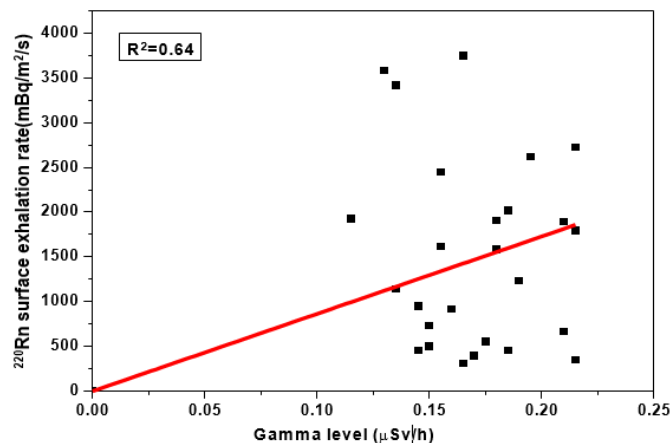
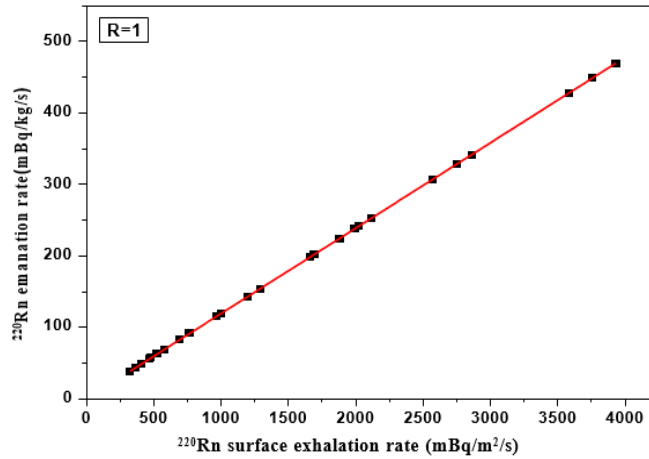


Fig. 1.13: Relationship b/w <sup>220</sup>Rn surface outbreak and  $\gamma$ -level

**<sup>220</sup>Rn exhalation rate and <sup>220</sup>Rn mass emanation rate**

Table 4.1 shows the <sup>220</sup>Rn mass emanation rates (mBq/kg/s) from various soil samples collected from different locations. The emanation coefficient varied from 39 to 470 mBq/kg/s

with average  $192 \pm 112$  mBq/kg/s. A correlation graph between <sup>220</sup>Rn mass emanation rate and exhalation rate is shown in Fig (4.14). It shows a strong positive correlation with  $R = 1$  as expected <sup>220</sup>Rn mass emanation rate is observed to be higher where <sup>220</sup>Rn exhalation rate is higher (Table 4.1).



**Fig. 1.14: Connection between exterior outbreath and discharge rate of <sup>220</sup>Rn**

In the Muzaffarnagar area, <sup>226</sup>Ra, <sup>232</sup>Th and <sup>40</sup>K levels in soil samples ranged from  $31 \pm 8$  Bqkg<sup>-1</sup> to  $63 \pm 10$  Bqkg<sup>-1</sup> with mean values of 48 Bqkg<sup>-1</sup> and  $25 \pm 7$  Bqkg<sup>-1</sup> to 57 Bqkg<sup>-1</sup>. varies from  $\pm 9$  Bqkg<sup>-1</sup> and  $1536 \pm 196$  Bqkg<sup>-1</sup> with a mean of 39 Bqkg<sup>-1</sup> to  $2261 \pm 287$  Bqkg<sup>-1</sup> with a mean of 1962 Bqkg<sup>-1</sup>. There is also a strong correlation between the mass ejection rate of <sup>222</sup>Rn and its radium content (correlation coefficient  $R^2 = 0.78$ ), as shown in Figure 1.15. Similar observations were found for the surface release rate of <sup>220</sup>Rn and its thorium content (correlation coefficient  $R^2 = 0.72$ ), as shown in Figure 1.16. This is also due to their stratification and the high mobility of <sup>222</sup>Rn and <sup>220</sup>Rn gases to the surface. The average values of <sup>226</sup>Ra and <sup>232</sup>Th in this region were slightly above the global average. H. 50 BqKg<sup>-1</sup> or 10-50 BqKg<sup>-1</sup>. The study area average of 40,000 exceeds the limit given by UNSCEAR (2000). H. 100-700 Bqkg<sup>-1</sup>. Radium

equivalent radioactivity (Raeq) was found to vary between 208 Bqkg<sup>-1</sup> and 311 Bqkg<sup>-1</sup> with an average value of 255 Bqkg<sup>-1</sup>. The average radium equivalent radioactivity was below the recommended value of 370 Bqkg<sup>-1</sup> (OECD, 1979). These high values of <sup>226</sup>Ra, <sup>232</sup>Th, and <sup>40</sup>K are associated with uranium, thorium mineralization, and the presence of highly mylonitized porphyry, granite, quartz porphyry, shale, phyllite schist, and quartzite belts. , which generally indicate higher radiation exposures on Earth. Muzaffarnagar district. External and internal health hazard index scores were found to be 0.56 to 0.84, mean scores 0.69, 0.67 to 1.00, mean scores 0.82, respectively. The region was found to have an average external and internal health hazard index of less than 1. This is very satisfactory and within the protected boundaries of the study area (UNSCEAR 1993; 2000).

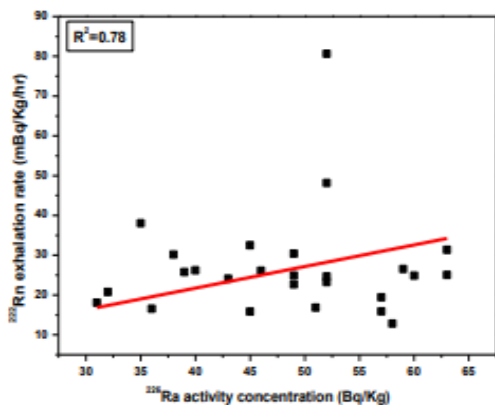


**Fig. 1.15: Correlation between <sup>222</sup>Rn mass exhalation rate and its Radium content**

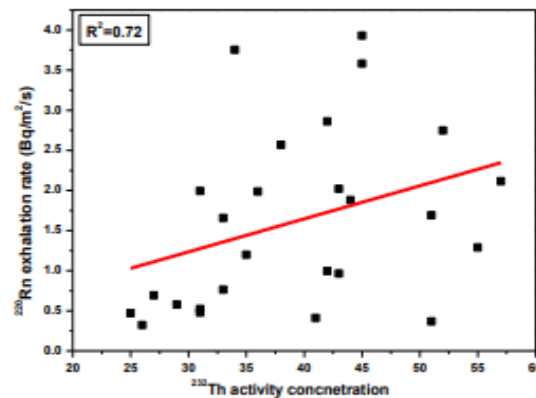


**Fig. 1.16: Correlation between <sup>220</sup>Rn surface exhalation rate and its Thorium content**

Table 1.4: 226Ra, 232Th, 40K radionuclides and measured annual effective doses in soil samples (Muzaffarnagar district)

Location Code	Activity Concentration Bqkg <sup>-1</sup> (concentration± error)			Ra <sub>eq</sub> (Bqkg <sup>-1</sup> )	Health Hazard Index		Absorbed Dose (nGyh <sup>-1</sup> )	Annual Effective Dose (mSv)	
	226Ra	232Th	40K		H <sub>ex</sub>	H <sub>in</sub>		Indoor	Outdoor
Badhiwala	52±9	55±9	1949±278	281	0.76	0.90	138.52	0.68	0.17
Akbargarh	63±10	43±8	1994±259	278	0.75	0.92	138.23	0.68	0.17
Dhudhli	52±11	35±7	2013±259	257	0.69	0.83	129.11	0.63	0.16
Ali Pura	51±9	45±8	2061±265	274	0.74	0.88	136.69	0.67	0.17
Almaspur	58±10	51±9	2261±287	305	0.82	0.98	151.88	0.75	0.19
Badheri	52±9	38±8	2098±268	268	0.72	0.86	134.46	0.66	0.16
Badiwala	49±9	43±8	2098±268	276	0.74	0.88	138.06	0.68	0.17
Baghra	52±9	44±9	2034±263	272	0.73	0.87	135.42	0.66	0.17
Bagowali	60±10	42±8	2170±277	287	0.78	0.94	143.58	0.70	0.18
Tugalakpur	32±8	26±7	2087±264	230	0.62	0.71	117.52	0.58	0.14
Khorkee	31±8	25±7	1942±249	216	0.58	0.67	110.40	0.54	0.14
Balwakheri	46±8	42±8	1971±254	258	0.70	0.82	128.81	0.63	0.16
Bamanheri	45±8	41±7	1563±196	224	0.60	0.73	110.73	0.54	0.14
Charthawal Rural	36±8	29±8	1857±261	220	0.60	0.69	111.58	0.55	0.14
Dadupur	57±9	51±7	1844±245	272	0.73	0.89	134.03	0.66	0.16
Dhandhera	37.6±9	31±11	2100±260	244	0.66	0.76	123.85	0.61	0.15
Dhudhli	35±9	33±11	2100±260	218	0.59	0.68	109.45	0.54	0.13
Faridpur	40±8	27±7	1955±251	229	0.62	0.73	116.31	0.57	0.14
Jaroda	49±8	34±7	1854±170	240	0.65	0.78	120.49	0.59	0.15
Kalewala	57±13	45±8	1825±181	262	0.71	0.86	129.62	0.64	0.16
Lakhnauti	45±8	31±7	1536±196	208	0.56	0.68	103.57	0.51	0.13
Mandi	63±10	52±8	2001±261	291	0.79	0.96	143.96	0.71	0.18
Mirzapur	59±10	57±9	2215±284	311	0.84	1.00	154.05	0.76	0.19
Nuna Khera	49±9	36±8	2075±264	260	0.70	0.84	130.91	0.64	0.16
Pilakhni	43±9	33±7	1922±248	238	0.64	0.76	119.95	0.59	0.15
Shahpur	39±8	31±7	1773±232	220	0.59	0.70	110.68	0.54	0.14

On the other hand, one sample (MBT area) shows a health hazard index higher than 1. The total absorbed dose rate was found to vary between 104 nGyh<sup>-1</sup> and 154 nGyh<sup>-1</sup> with an average value of 128 nGyh<sup>-1</sup> due to the presence of 226Ra, 232Th and 40K in soil samples. Average absorbed dose rates in the study area were found to be higher than recommended. H. 60 nGyh<sup>-1</sup> (UNSCEAR, 2000). The total indoor effective dose ranged from 0.51 mSvy<sup>-1</sup> to 0.76 mSvy<sup>-1</sup> with a mean value of 0.63 mSvy<sup>-1</sup>, and the total outdoor effective dose ranged from 0.13 mSvy<sup>-1</sup> to 0.19 mSvy<sup>-1</sup> with a mean variation of Average 0.16 mSvy<sup>-1</sup>. The slightly higher concentration of 226Ra in the study area (Muzaffarnagar) may be due to the presence of uranium-rich thorium ores deposited in the rocks of the study area. The Muzaffarnagar region is a Thrust and Neotect region. UNSCEAR reports that 40K, 238U, and 232Th account for 35, 25, and 40%, respectively, of the total radiation dose to which the population is exposed (UNSCEAR 1982). Soil and rocks are one of the main sources of this background radiation. Radionuclides present in rocks are carried to soil by rain and subsequent water flow (Taskin et al. 2009). Therefore, once reached, these radionuclides somehow remain in the soil. The high uranium content of mineralized granites and phosphates

is attributed to the availability of iron oxide as absorbed uranium from the circulating solution or to the preponderance of oxidizing conditions. A variety of commonly found granular flat phosphates, composed of fragments of associated rock units, suggest simultaneous transport and turbulence within the basin. Uranium in these phosphate deposits appears to be absorbed in cellophane and phosphate matrices. Radioactivity variability strongly depends on the geological conditions of the study area and the composition of the rock formations in this area (Choubey et al., 1999). These results are also important for environmental studies, as local soils in hilly areas are used for a variety of purposes in mud buildings. External and internal health hazard indices were calculated from the measured radioactivity in terms of radiation protection.

### Conclusion

Results obtained from these study areas (Muzaffarnagar district) show that all calculated parameters of expiratory velocity, radiation injury and dose for 222Rn and 220Rn are well below the values proposed for estimating stable source terms. indicates that it is within range. Expiratory rates of

222Rn and 220Rn were measured using the chamber technology supported by the Smart RnDuo portable monitor. Basically, the release rates of 222Rn and 220Rn depend on two factors: 1) 226Ra and 232Th contents in soil, and 2) geographical distribution and soil composition. Higher than global average soil 226Ra, 232Th, and 40K levels (with the exception of a few locations) and relatively high values of 222Rn and 220Rn expiratory rates are consistent with indoor 222Rn and 220Rn concentrations reported in these regions. confirms the observations. The correlations between expiratory rates of 222Rn and 220Rn and gamma levels with expiratory rates of 222Rn and 220Rn were found to be weak in the Muzaffarnagar area due to the random distribution of source terms and soil composition. The 220Rn exhalation is much higher in the Basoli area (Muzaffarnagar district) with higher grades of thorium, strata and phosphate rocks consisting of uranium mineralization. A strong positive correlation between 222Rn/220Rn expiratory rate and gamma

levels in the Muzaffarnagar region concludes that the surface flux was equally contributed by 222Rn/220Rn expiratory rate and gamma levels. The high levels of natural radionuclides in the study area may be due to the combined effects of radionuclide mineral abundance and the presence of a nearby thrust zone. Absorbed doses were higher than the world average, but annual absorbed doses were below recommended values. The internal and external health hazard index and gamma index were below the recommended value of 1. It is known that soils from various strata in Muzaffarnagar district can be safely used for building materials and other purposes without causing radiation hazards to residents. This study can be used to calculate emissivity in these regions, an important parameter in modeling radon levels in soil gases, outdoor and indoor air. The results of the current study will help bridge the source terms, contributing factors and concentration values of the study area that are important for future research expeditions.

## References

1. Aldenkamp FJ, De Meijer RJ, Put LW, Stoop P. An assessment of in situ radon exhalation measurements, and the relation between free and bound exhalation rates. *Radiat Prot Dosim* 1992;45(1-4):449-453
2. Bossew P, Lettner H. Investigations on indoor radon in Austria, Part 1: Seasonality of indoor radon concentration. *J Environ Radioact* 2007;98(3):329-45.
3. Chau ND. Factors controlling measurements of radon mass exhalation rate. *J Environ Radioact* 2005;82:363-369.
4. Darby S, Hill D, Auvinen A, Barros-Dios JM, Baysson H, Bochicchio F, Deo H, Falk R, Forastiere F, Hakama M, Heid I. Radon in homes and risk of lung cancer: Collaborative analysis of individual data from 13 European case-control studies. *BMJ* 2005;330(7485):223-226.
5. Diab HM, Nouh SA, Hamdy A, El-Fiki SA. Evaluation of natural radioactivity in a cultivated area around a fertilizer factory. *J Nucl Rad Phys* 2008;3(1):53-62.
6. Eappen KP, Mayya YS, Patnaik RL, Kushwaha HS. Estimation of radon progeny equilibrium factors and their uncertainty bounds using solid state nuclear track detectors. *Radiat Meas* 2006;41: 342-348.
7. Etiope G, Martenelli G. Migration of carrier and trace gases in the geosphere: an overview. *Phys. Earth Planet Inter* 2002;129:185-204.
8. Gaware JJ, Sahoo BK, Sapra BK, Mayya YS. Development of online radon and thoron monitoring systems for occupational and general environments. *BARC News Lett* 2011;318: 45-51
9. Gregoric A, Vaupotic J, Kardos R, Horvath M, Bujtor T, Kovacs T. Radon emanation of soils from different lithological units. *Carpathian J Earth Environ Scien* 2013;8(2): 185-190.
10. Ibrahim N. Natural radioactivity of 238U, 232Th and 40K in building materials. *J Environ Radiact* 1999;43:255-258.
11. Jelle BP. Development of a model for radon concentration in indoor air. *Sci Total Environ* 2012;416:343-350.
12. Johner HUU, Surbeck H. Soil gas measurements below foundation depth improve indoor radon prediction. *Sci Total Environ* 2001;272(1-3):337-341
13. Kant K, Sonkawade RG, Sharma GS, Chauhan RP, Chakarvarti SK. Seasonal variation of radon, thoron and their progeny levels in dwellings of Haryana and Western Uttar Pradesh. *Int J Radiat Res* 2009;7(2):79.
14. Kardos R.A, Gregoric J, Jonas J, Vaupotic T, Kovacs Y, Ishimori. Dependence of radon emanation of soil on lithology. *J. Radio analytical Nucl Chem.* 2015;304:1321-1327.
15. Krewski D, Lubin JH, Zielinski JM, Alavanja M, Catalan VS, Field RW, Klotz JB, Le´tourneau EG, Lynch CF, Lyon JL, Sandler DP, Schoenberg JB, Steck DJ, Stolwijk JA, Weinberg C, Wilcox HB. Residential radon and risk of lung cancer: a combined analysis of 7 North American case-control studies. *Epidemiology* 2005;16(2):137-145
16. Kumar A, Chauhan RP, Joshi M, Sahoo BK. Modeling of indoor radon concentration from radon exhalation rates of building materials and validation through measurements. *J Environ Radioact* 2014;127: 50-55.
17. Mayya YS. Theory of Radon exhalation into Accumulators placed at the soil-atmosphere interface. *RadiatProtDosim*2004;3(3):305-318.
18. Prasad G, Prasad Y, Gusain GS, Ramola RC. Measurement of radon and thoron levels in soil, water and indoor atmosphere of Budhakedar in Garhwal Himalaya, India. *Radiat Meas* 2008;43:375-379.
19. Prasad Y, Prasad G, Gusain GS, Choubey VM, Ramola RC. Radon exhalation rate from soil samples of South Kumaun Lesser Himalayas, India. *Radiation Measurements* 2008;43:369-374
20. Ramola RC, Prasad G, Gusain GS, Rautela BS, Choubey VM, Sagar DV, Tokonami S, Sorimachi A, Sahoo SK, Janik M, Ishikawa T. Preliminary indoor thoron measurements in high radiation background area of southeastern coastal Orissa, India. *Radiat Prot Dosim* 2010;141:379-382
21. Ramola RC, Prasad M, Kandari T, Pant P, Bossew P, Mishra R, Tokonami S. Dose estimation derived from the exposure to radon, thoron and their progeny in the indoor environment. *Scientific Reports* 2016;6:31061.

22. Ramola RC, Rautela BS, Gusain GS, Prasad G, Sahoo SK, Tokonami S. Measurements of radon and thoron concentrations in high radiation background area using pin-hole dosimeter. *Radiat Meas* 2013;53-54:71-73.
23. Roelofs LM, Scholten LC. The effect of aging, humidity, and fly-ash additive on the radon exhalation from concrete. *Health phys* 1994 ;67(3):266-71.
24. Ryzhakova NK. A new method for estimating the coefficients of diffusion and emanation of radon in the soil. *J. Environ. Radioact.* 2014 ;135:63-6.
25. Sahoo BK, Mayya YS. Two dimensional diffusion theory of trace gas emission into soil chambers for flux measurements. *Agric. For. Meteorol.* 2010;150:1211-1224.
26. Sahoo BK, Sapra BK, Gaware JJ, Kanse SD, Mayya YS. A model to predict radon exhalation from walls to indoor air based on the exhalation from building material samples. *Sci Total Environ* 2011;409:2635-2641.
27. Singh K, Semwal P, Pant P, Gusain GS, Joshi M, Sapra BK, Ramola RC. Measurement of radon, thoron and their progeny in different types of dwelling in Almora district of Kumaun Himalayan region. *Radiat Prot Dosim* 2016;171: 223-228.
28. Stoulos S, Manolopoulou M, Papastefanou C. Assessment of natural radiation exposure and radon exhalation from building materials in Greece. *J. Environ. Radioact.* 2003;69(3):225-40
29. Strandén E, Kolstad AK, Lind B. The influence of moisture and temperature on radon exhalation. *Radiat. Prot. Dosimetry.* 1984;7(1-4):55-8.
30. Teras LR, Diver WR, Turner MC, Krewski D, Sahar L, Ward E, Gapstur SM. Residential radon exposure and risk of incident hematologic malignancies in the Cancer Prevention Study-II Nutrition Cohort. *Environ. Res.* 2016;148:46-54.
31. Tripathi RM, Sahoo SK, Jha VN, Khan AH, Puranik VD. Assessment of environmental radioactivity at uranium mining, processing and tailings management facility at Jaduguda, India. *Appl. Radiat. Isot.* 2008;66(11):1666-70.
32. UNSCEAR. Effects and Risks of Ionizing Radiation. 1993 United Nations, New York
33. UNSCEAR. Sources and effects of ionizing radiation 2009.
34. UNSCEAR. Sources and Effects of Ionizing Radiation. 2010 United Nations, New York.
35. UNSCEAR. Sources, effects and risk of ionizing radiation, Report to the General Assembly, United Nations, New York 2000.